This is the accepted manuscript made available via CHORUS. The article has been published as:

Analytical WKB theory for high-harmonic generation and its application to massive Dirac electrons

Hidetoshi Taya, Masaru Hongo, and Tatsuhiko N. Ikeda

Phys. Rev. B **104**, L140305 — Published 21 October 2021

DOI: 10.1103/PhysRevB.104.L140305

Analytical WKB theory for high-harmonic generation and its application to massive Dirac electrons

Hidetoshi Taya,[1,2,*] Masaru Hongo,[3,1,†] and Tatsuhiko N. Ikeda[4,‡]

[1] *RIKEN iTHEMS, RIKEN, Wako 351-0198, Japan*
[2] *Research and Education Center for Natural Sciences, Keio University 4-1-1 Hiyoshi, Kohoku-ku, Yokohama, Kanagawa 223-8521, Japan*
[3] *Department of Physics, University of Illinois, Chicago, Illinois 60607, USA*
[4] *Institute for Solid State Physics, University of Tokyo, Kashiwa, Chiba 277-8581, Japan*

(Dated: October 7, 2021)

We propose an analytical approach to high-harmonic generation (HHG) for nonperturbative low-frequency and high-intensity fields based on the (Jeffreys-)Wentzel-Kramers-Brillouin (WKB) approximation. By properly taking into account Stokes phenomena of WKB solutions, we obtain wavefunctions that systematically include repetitive dynamics of production and acceleration of electron-hole pairs and quantum interference due to phase accumulation between different pair production times (Stückelberg phase). Using the obtained wavefunctions without relying on any phenomenological assumptions, we explicitly compute electric current (including intra- and inter-band contributions) as the source of HHG for a massive Dirac system in (1+1)-dimensions under an ac electric field. We demonstrate that the WKB approximation agrees well with numerical results obtained by solving the time-dependent Schrödinger equation and point out that the quantum interference is important in HHG. We also predict in the deep nonperturbative regime that (1) harmonic intensities oscillate with respect to electric-field amplitude E_0 and frequency Ω, with a period determined by the Stückelberg phase; (2) cutoff order of HHG is determined by $2eE_0/\hbar\Omega^2$, with e being the electron charge; and that (3) non-integer harmonics, controlled by the Stückelberg phase, appear as a transient effect. Our WKB theory is particularly suited for a parameter regime, where the Keldysh parameter $\gamma = (\Delta/2)\Omega/eE_0$, with Δ being the gap size, is small. This parameter regime corresponds to intense lasers in the terahertz regime for realistic massive Dirac materials. Our analysis implies that the so-called HHG plateau can be observed at the terahertz frequency within the current technology.

Introduction.— High-harmonic generation (HHG) is one of the most intriguing phenomena in nonlinear optics [1]. Thanks to developments in laser technologies over the decades, HHG has been observed and analyzed in various media (e.g., atomic gases [2–4], liquids [5, 6], semiconductors [7–11], graphene [12–15], superconductors [16–19], strongly-correlated electrons [20–23], and amorphous solids [24, 25]), providing a unique opportunity to explore the fully nonperturbative regime of matter-field interaction and rich applications such as attosecond light sources and ultrafast imaging methods [26]. HHG has also been predicted in the fundamental theory of quantum electrodynamics (QED), i.e., the QED vacuum emits high harmonics when exposed to strong fields exceeding the Schwinger limit [27, 28].

One of the greatest theoretical challenges to elucidate the HHG mechanism is to understand nonperturbative electron dynamics under low-frequency and high-intensity fields [29, 30]. Typically, theorists numerically solve the time-dependent Schrödinger equation (TDSE) [31–33] (or von Neumann equation [34–37]) to simulate electric current and/or polarization as the source of HHG. These studies have provided numerical evidence that the interplay between the intra- and inter-band electron dynamics plays an essential role. Meanwhile, analytical methods are demanded to deepen the fundamental understanding and to analyze numerically inaccessible parameter regimes such as the low-frequency limit. Analytical theories exist for the simplest single-band model [7, 38], which, however, completely neglects the interband dynamics. For multiband models, there are Floquet-theoretical approaches [39, 40], but analytical results have been limited to the high-frequency regime where the laser frequency Ω exceeds the band gap Δ. Thus, analytical HHG theory has not been established for the quintessential low-frequency and high-intensity fields.

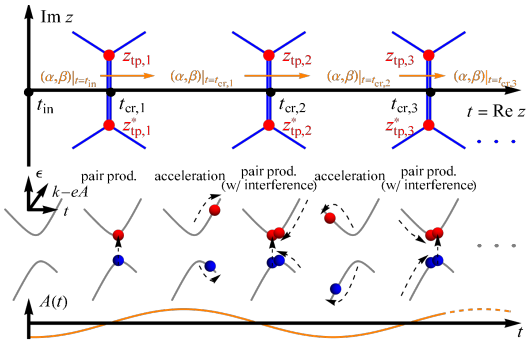


FIG. 1. (a) A typical Stokes graph, composed of Stokes lines (blue lines) and turning points (red points), and (b) the corresponding physical processes during the real-time evolution.

In this Letter, we present an analytical method to

* hidetoshi.taya@riken.jp
† masaru.hongo@riken.jp
‡ tikeda@issp.u-tokyo.ac.jp

study HHG in the nonperturbative low-frequency and high-intensity regime. Our method is based on (Jeffreys-)Wentzel-Kramers-Brillouin ((J)WKB [41–44]) approximation, which has been extended by mathematicians since 1980's (leading to the exact WKB analysis) [45–52] and applied successfully to various physical problems such as tunneling pair production [53–57] and nonlinear radiative processes under strong fields [58–60]. The WKB approximation is a semi-classical method valid in the formal limit $\hbar \to 0$ or equivalently when the Keldysh parameter [55, 61–64]

$$\gamma \equiv \frac{\Omega(\Delta/2)}{eE_0} \tag{1}$$

is sufficiently small (e and E_0 are electron charge and electric-field amplitude, respectively, and we assume $eE_0 > 0$ and set the speed of light to be unity). Hence, it is suited for low-frequency and high-intensity fields, where nonperturbative processes, such as quantum tunneling (Landau-Zener transition [65–68] or Sauter-Schwinger effect [69–71]), take place. Another advantage is that one can explicitly solve TDSE (up to some order of $\hbar$) and can compute observables directly from the wavefunction without any ad-hoc assumptions. The wavefunction has microscopic information on the nonperturbative electron-hole dynamics under strong fields, which enables us to understand the HHG mechanism.

Setup.— For concreteness, we consider massive Dirac electrons in (1+1)-dimensions under a time-dependent electric field $E(t)$. The Hamiltonian reads

$$H \equiv \begin{pmatrix} \Delta/2 & k - eA \\ k - eA & -\Delta/2 \end{pmatrix}, \tag{2}$$

where $A(t) \equiv -\int^t \mathrm{d}t'\, E(t')$ is the vector potential, k is canonical momentum (or Bloch momentum in solids), and Δ is the gap energy. Note that the Hamiltonian (2) is relativistic and linear in k, so that the diamagnetic term A^2 is absent unlike non-relativistic Hamiltonians. The following argument also applies to general two-level systems, e.g., Dirac materials (including QED) in other dimensions [72], topological insulators [73], semiconductors [29], and graphene [74, 75]. We assume that the electric field is turned on at $t = t_{\rm in}$, before which the system is in the ground state, and compute the induced electric current as the source of HHG. As we will clarify soon, our WKB theory is valid in the non-perturbative regime $\gamma \lesssim 1$. For realistic massive Dirac materials $\Delta = \mathcal{O}(10\,\mathrm{meV})$ [76, 77], this corresponds to intense ($E_0 \gtrsim 1\,\mathrm{kV/cm}$) terahertz [$\Omega/(2\pi) \sim 10^{12}\,\mathrm{Hz}$] lasers, which are available within the current laser technology used in the terahertz HHG observations [15, 78, 79].

WKB solution and Stokes phenomenon.— To solve TDSE with the Hamiltonian (2), we expand the solution ψ by WKB wavefunctions $\psi_\pm$,

$$\psi(t) = \alpha\psi_-(t) + \beta\psi_+(t), \tag{3}$$

where α and β are called Stokes constants and satisfy $1 = |\alpha|^2 + |\beta|^2$ so that $1 = \psi^\dagger\psi$. We work within the lowest-order WKB approximation, where $\psi_\pm$ is given by the instantaneous eigenstates for the Hamiltonian (2) with dynamical phase factors:

$$\begin{aligned}
\psi_+ &= \frac{1}{\sqrt{2}}\sqrt{1 - \frac{\Delta/2}{\epsilon}} \begin{pmatrix} +\frac{k-eA}{\epsilon-\Delta/2} \\ 1 \end{pmatrix} \mathrm{e}^{-\frac{\mathrm{i}}{\hbar}\int_0^t \mathrm{d}t\,\epsilon}, \\
\psi_- &= \frac{1}{\sqrt{2}}\sqrt{1 - \frac{\Delta/2}{\epsilon}} \begin{pmatrix} 1 \\ -\frac{k-eA}{\epsilon-\Delta/2} \end{pmatrix} \mathrm{e}^{+\frac{\mathrm{i}}{\hbar}\int_0^t \mathrm{d}t\,\epsilon},
\end{aligned} \tag{4}$$

with $\epsilon \equiv \sqrt{(\Delta/2)^2 + (k - eA)^2}$ being the instantaneous eigenenergy, which includes the intraband acceleration by the external field.

To determine the Stokes constants α and β, we analytically continue the instantaneous energy onto the complex z-plane $\epsilon(t \in \mathbb{R}) \to \epsilon(z \in \mathbb{C})$ and analyze the associated Stokes graph (see Fig. 1). The Stokes constants α and β take constant values within each Stokes region, which is defined as a region in the complex z-plane separated by Stokes lines $\mathcal{C}_{z^{\rm tp}} \equiv \{z \in \mathbb{C} \mid 0 = \mathrm{Im}[\frac{\mathrm{i}}{\hbar}\int_{z^{\rm tp}}^z \mathrm{d}z\,\epsilon]\}$, with $z^{\rm tp} \in \mathbb{C}$ being turning points such that $0 \equiv \epsilon(z^{\rm tp})$. For the instantaneous energy ϵ that are real on the real axis, turning points and Stokes lines are symmetric in the upper and lower complex z-planes, and the pairs of turning points $(z^{\rm tp}, z^{\rm tp*})$ are connected with a doubly degenerated Stokes line crossing the real axis only once at $t^{\rm cr} = \{t \in \mathbb{R} \,|\, 0 = \mathrm{Im}[\frac{\mathrm{i}}{\hbar}\int_{z^{\rm tp}}^t \mathrm{d}z\,\epsilon]\}$ [55]. Whenever $t \in \mathbb{R}$ crosses a degenerated Stokes line at $t = t^{\rm cr}$ during the time-evolution, the Stokes constants α and β jump discontinuously (Stokes phenomenon) as [55, 80]

$$\begin{pmatrix} \alpha \\ \beta \end{pmatrix}\Big|_{t_n^{\rm cr}+0^+} = \begin{pmatrix} 1 & (-1)^n \mathrm{e}^{-\frac{\sigma_n^*}{\hbar}} \\ -(-1)^n \mathrm{e}^{-\frac{\sigma_n}{\hbar}} & 1 \end{pmatrix} \begin{pmatrix} \alpha \\ \beta \end{pmatrix}\Big|_{t_n^{\rm cr}-0^+}, \tag{5}$$

where $\sigma_n \equiv 2\mathrm{i}\int_0^{z_n^{\rm tp}} \mathrm{d}z\,\epsilon$ ($\mathrm{Re}\,\sigma_n > 0$), $t_n^{\rm cr}$ ($t^{\rm in} < t_1^{\rm cr} < t_2^{\rm cr} < \cdots$) is the n-th crossing associated with $(z_n^{\rm tp}, z_n^{\rm tp*})$, and we neglected subleading $\mathcal{O}(\mathrm{e}^{-\frac{2}{\hbar}\mathrm{Re}\,\sigma_n})$ terms by assuming $\hbar \to 0$. Using Eq. (5), we find an approximate solution, starting from the initial ground-state wavefunction $(\alpha, \beta)|_{t=t^{\rm in}} = (1, 0)$, as

$$\psi = \psi_- - \sum_n (-1)^n \mathrm{e}^{-\frac{\sigma_n}{\hbar}} \Theta(t - t_n^{\rm cr})\psi_+. \tag{6}$$

The Stokes constant β (5) [i.e., the coefficient in front of ψ_+ in Eq. (6)] gives the probability amplitude from the initial ground state to an excited state with the instantaneous basis (4). Thus, $\beta \neq 0$ means electron-hole pair production occurs (see Fig. 1), and $|\beta|^2$ gives the pair production number. The typical magnitude of the production number is determined by the exponential factor $\mathrm{e}^{-\frac{1}{\hbar}\mathrm{Re}\,\sigma_n}$. Note that Eq. (6) takes the form of superposition of the wavefunctions describing the pair production at different times. The phase factor $\mathrm{e}^{-\frac{\mathrm{i}}{\hbar}\mathrm{Im}\,\sigma_n}$, related to the so-called Stückelberg phase, is thus responsible for

quantum interference effect [67, 80–82]: When pair production occurs repetitively, the Stückelberg phase, i.e., the relative phase between each wavefunction

$$\theta_{n,n'} \equiv \frac{2}{\hbar}\int_{t^{\rm cr}_{n'}}^{t^{\rm cr}_{n}} {\rm d}t\,\epsilon = -\frac{1}{\hbar}({\rm Im}\,\sigma_n - {\rm Im}\,\sigma_{n'}) \neq 0, \tag{7}$$

gives rise to destructive and constructive interferences, which suppress and enhance the production, respectively. Note that our Stokes constants α and β (5) neglect pair annihilation processes followed after the production, which are higher order effects $\mathcal{O}(\mathrm{e}^{-\frac{2}{\hbar}{\rm Re}\,\sigma_n})$.

Within the lowest-order WKB approximation (4), the production number $|\beta|^2$ shows stepwise time-dependence, meaning that each production process is treated as instantaneous one that occurs exactly at $t = t^{\rm cr}_n$. In reality, the stepwise evolution is an approximation, and pair production takes finite time $\delta t \neq 0$. Under an electric field, for a pair production to occur via quantum tunneling, an electron in the valence-band needs to tunnel a distance $\sim \Delta/eE_0$ to the conduction-band, and hence $\delta t \sim \gamma\Omega^{-1}$ with the Keldysh parameter γ. Thus, the WKB approximation would not work for very high harmonics $N \equiv \omega/\Omega \gtrsim (2\pi/\delta t)/\Omega \sim 2\pi\gamma^{-1}$ or when $\gamma \gtrsim 2\pi/N$. This also implies that the WKB approximation cannot describe perturbative excitation processes, which dominate for large γ [55, 61–64].

WKB result for electric current.— We compute the electric current $J \equiv \langle -\delta H/\delta A\rangle = e\psi^\dagger\sigma^1\psi$ at each momentum k. The WKB approximation (6) gives J as a sum of the valence-, intra-, and inter-band contributions, $J = J_{\rm val} + J_{\rm intra} + J_{\rm inter}$, where

$$J_{\rm val} \equiv e\psi_-^\dagger\sigma^1\psi_- = -ev, \tag{8}$$

$$J_{\rm intra} \equiv \sum_{\pm}|\beta|^2(\pm e)\psi_\pm^\dagger\sigma^1\psi_\pm = 2ev\left|\sum_n(-1)^n\mathrm{e}^{-\frac{\sigma_n}{\hbar}}\Theta(t-t^{\rm cr}_n)\right|^2,$$

$$J_{\rm inter} \equiv 2e\,{\rm Re}\left(\alpha\beta^*\psi_+^\dagger\sigma^1\psi_-\right) = e\frac{\Delta}{\epsilon}\sum_n(-1)^n\mathrm{e}^{-\frac{1}{\hbar}{\rm Re}\,\sigma_n}\Theta(t-t^{\rm cr}_n)\cos\left(\frac{2}{\hbar}\int_{t^{\rm cr}_n}^{t}{\rm d}t\,\epsilon\right),$$

with velocity $v \equiv (k - eA)/\epsilon$. Being proportional to v, $J_{\rm val}$ ($J_{\rm intra}$) is accompanied by valence-band electrons (electron-hole pairs) accelerated along the band(s). $J_{\rm inter}$ originates from interference between conduction- and valence-band electrons (or dipole [83]), as is evident from the wavefunction overlap ${\rm Re}(\alpha\beta^*\psi_+^\dagger\sigma^1\psi_-)$. Since the actual observable is the difference from the ground state, we subtract $J_{\rm val}$ and focus on

$$J_{\rm obs} \equiv J - J_{\rm val} = J_{\rm intra} + J_{\rm inter}. \tag{9}$$

This is a standard subtraction scheme widely used in quantum-field theory in external fields [84]. Also, in the condensed-matter context, the subtracted $J_{\rm val}$ amount to be zero when summed over the entire Brillouin zone.

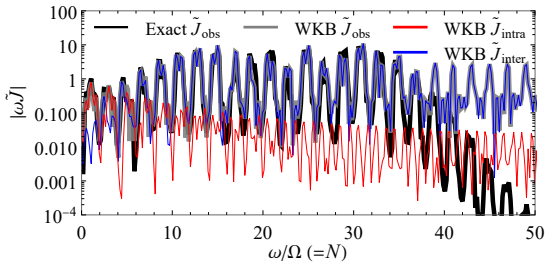


FIG. 2. HHG spectrum for the oscillating field (10), with $\Omega/(\Delta/2) = 1/4$, $eE_0/(\Delta/2)^2 = 1$ (i.e., $\gamma = 1/4$) and $\Omega t_{\rm in} = -17\pi/3$, $T_w = 2|t_{\rm in}|$. The parameter set corresponds to, e.g., $\Omega/2\pi = 1\,$THz and $E_0 = 4.2\,$kV/cm for a Dirac material with Fermi velocity $v_{\rm F} = 10^6\,$m/s and mass $\Delta = 33\,$meV.

Note that the observable currents, $J_{\rm intra}$ and $J_{\rm inter}$, reproduce the phenomenological expressions used in previous studies on semi-conductor HHG [36, 37].

According to Eq. (8), the nonlinear response to the applied field arises not only from the pair production factor $\mathrm{e}^{-\frac{\sigma_n}{\hbar}}$ but also from the velocity v in $J_{\rm intra}$. Whereas the nonlinearity of v is absent for the quadratic dispersion, it can be significant for the linear one in massless Dirac systems [78, 79, 85]. The strong nonlinearity survives to some extent even in our massive case.

HHG by ac electric field.— As a demonstration, we consider a monochromatic ac field,

$$eA = -\frac{eE_0}{\Omega}\sin(\Omega t), \tag{10}$$

and take $k \to 0$, as pair production at large k may be energetically disfavored (see Ref. [86] for situations where various k's become important). For the field (10), the wavefunction encounters two crossings in a cycle $t^{\rm cr}_n \in \frac{\pi}{\Omega}\mathbb{Z}$, i.e., pairs are produced twice in a cycle. This is similar to the three-step process in the gas HHG [3, 4]. Although our WKB approach also applies to other k's, their analytical expressions become more complex. We leave, for future work, this generalization and summing the results over k's. In exchange for restricting ourselves to $k \to 0$, we will obtain analytical closed formulas, which would at least qualitatively capture the HHG in the massive Dirac electrons.

We compute the Fourier spectrum of the observable $\tilde{J}_{\rm obs} \equiv \int_{-\infty}^{+\infty}{\rm d}t\,\mathrm{e}^{+{\rm i}\omega t}WJ_{\rm obs} = \tilde{J}_{\rm intra} + \tilde{J}_{\rm inter}$, where we insert a window function W with width T_w to avoid contaminations due to finiteness of fields/measurements [31, 87]. Here, we chose the Hann window $W \equiv \Theta(t - t_{\rm in})\Theta(T_w + t_{\rm in} - t)\sin^2(\pi(t - t_{\rm in})/T_w)$ and confirmed that the results are insensitive to the choice of W. One can obtain a closed analytical expression for $J_{\rm obs}$ under Eq. (10), from which one can compute the spectrum $\tilde{J}_{\rm obs}$ numerically or even analytically under certain approximations [88].

The HHG spectrum obtained from the WKB approximation (8) agrees well for small γ with the exact one obtained by numerically solving TDSE; see Fig. 2. Due to the limitation of the WKB approximation, the discrepancy for very high harmonics appears at $N \gtrsim 35$ in

Fig. 2, which is consistent with our estimate $\sim 2\pi\gamma^{-1}$.

Our WKB result confirms that the interband contribution dominates over the intraband one, except for the low harmonics ($N \lesssim 3$ in Fig. 2) [36, 37]. This means that the interband contribution is the origin of the plateau structure in the HHG spectrum [8]. One may estimate the location of the cutoff by using the saddle-point method [4, 36, 37] when evaluating the Fourier integral of the WKB expressions (8). The stationary conditions for the intra- and inter-band currents are given by $\omega = 0$ and $2\epsilon - \hbar|\omega| = 0$, respectively. The former condition confirms why the intraband current contributes only to the low harmonics. The latter condition can have real solutions when $\Delta/\hbar\Omega \lesssim N \lesssim \sqrt{\Delta^2 + 4(|k| + eE_0/\Omega)^2}/\hbar\Omega \sim 2(|k| + eE_0/\Omega)/\hbar\Omega$. If the stationary points are imaginary, the saddle-point action acquires positive real part and then the spectrum $\tilde{J}_{\rm inter}$ is suppressed exponentially. Therefore, it is sufficient to pick up the contribution from the real solution only, which yields that the upper cutoff of the HHG spectra for $k \to 0$ is given by

$$N_{\rm cut} \sim \frac{2eE_0}{\hbar\Omega^2} \tag{11}$$

(~ 32 in Fig. 2). The linear dependence on E_0 is consistent with semiconductor experiments [7], and the frequency dependence Ω^{-2} is our prediction in the massive Dirac electrons, which is worth testing in experiments (see Ref. [39] for a similar prediction in a charge-density-wave material). Note that the lower cutoff $N \sim \Delta/\hbar\Omega$ (~ 8 in Fig. 2) for the interband current is also consistent with Fig. 2.

To further investigate the HHG spectrum, we plot the eE_0- and Ω^{-1}-dependence of each harmonic intensity in Fig. 3. The WKB result reproduces the exact one in the nonperturbative high-intensity and low-frequency regime $\gamma \lesssim 2\pi/N$, while it fails for the perturbative low-intensity and high-frequency one $\gamma \gtrsim 2\pi/N$. In the perturbative regime, the N-th harmonic intensity shows power-dependence on the potential $(eA)^N \propto (eE_0/\Omega)^N$. This indicates that a perturbative N-photon process dominates, which cannot be captured by the WKB approximation. On the other hand, the harmonic intensities saturate (with oscillations) in the nonperturbative regime. The typical magnitude of the currents asymptote $|\tilde{J}_{\rm intra}| \to |\beta|^2 \propto \mathrm{e}^{-\pi\frac{(\Delta/2)^2}{eE_0}}$ and $|\tilde{J}_{\rm inter}| \to |\beta| \propto \mathrm{e}^{-\pi\frac{(\Delta/2)^2}{2eE_0}}$, which are independent of Ω and N. This explains why the harmonic intensities have weak N-dependence in the nonperturbative regime and the plateau appears in Fig. 2. Notice that the nonperturbative dependence on eE_0 is the manifestation that the production is driven by tunneling and agrees with the tunneling production formula [65–71].

The oscillating behavior in Fig. 3 is caused by the quantum interference. When the interference becomes destructive (constructive), the production and associated HHG are suppressed (enhanced). For our field (10) with the limit $k \to 0$, the Stückelberg phase can be decomposed as $\theta_{n,n'} = (n - n')\theta$, where $\theta \equiv \frac{2}{\hbar}\int_{t_n^{\rm cr}}^{t_{n+1}^{\rm cr}} \mathrm{d}t\, \epsilon = \frac{2}{\hbar}\int_0^{\pi/\Omega} \mathrm{d}t\, \epsilon$ is the phase for two successive production and is independent of n. Then, Eq. (5) indicates that the most destructive (constructive) interference occurs when θ matches even- (odd-) integer multiples of π. As shown analytically below, θ is roughly proportional to eE_0/Ω^2, and hence the harmonic intensities oscillate with eE_0 and Ω. This Stückelberg-phase mechanism for the oscillation is analogous to that in the gas HHG [89, 90] and would also apply to the recent semiconductor HHG experiment [91]. Note that we focus on $k \to 0$ although the physically-observed current are obtained in principle by collecting contributions from different k's over the Brillouin zone. Since the Stückelberg phase depends smoothly on k, the sum over k would smoothen the oscillating behavior in Fig. 3. As noted above, we leave it for future work to extend our analytical WKB theory for different k's.

Analytical formula in the low-frequency limit.— To get deeper insights, we analytically carry out the Fourier integration for the WKB result in the limit of $\gamma, k \to 0$ [88]:

$$\begin{aligned}
\tilde{J}_{\rm intra} &\sim \mathrm{e}^{-\frac{2\,\mathrm{Re}\,\sigma}{\hbar}} \frac{-\mathrm{i}}{\pi\cos^2\frac{\theta}{2}} \sum_{n=-\infty}^{\infty} \left[\sum_{\pm} \mathrm{e}^{+\mathrm{i}\pi\left(\left\lceil \frac{t_{\rm in}}{\pi/\Omega}\right\rceil - \frac{1}{2}\right)\left(\mp\frac{\theta}{\pi} - 1\right)} \frac{\sin\frac{\theta}{2}}{4\left(n - \frac{\theta}{2\pi}\right)} \tilde{W}\left(\omega - \Omega \mp 2\left(n - \frac{\theta}{2\pi}\right)\Omega\right) - \frac{\tilde{W}\left(\omega - (2n-1)\Omega\right)}{2n-1} \right], \\
\tilde{J}_{\rm inter} &\sim \mathrm{e}^{-\frac{\mathrm{Re}\,\sigma}{\hbar}} \frac{-\mathrm{i}(-1)^{\left\lceil \frac{t_{\rm in}}{\pi/\Omega}\right\rceil}\gamma}{4\pi\cos\frac{\theta}{2}} \sum_{n=-\infty}^{+\infty} \sum_{\pm} \left[\left(\ln\gamma^2 + 2H_{\pm n-1/2}\right) \mathrm{e}^{+\mathrm{i}\pi\left(\left\lceil \frac{t_{\rm in}}{\pi/\Omega}\right\rceil - \frac{1}{2}\right)\left(\mp\frac{\theta}{\pi} - 1\right)} \tilde{W}\left(\omega \mp 2\left(n - \frac{\theta}{2\pi}\right)\Omega\right) \right] \\
&\quad + \left(\ln(4\gamma^2) - \left((-1)^n\cos\frac{\theta}{2} - 1\right) H_{\frac{n}{2} \pm \frac{\theta}{4\pi} - 1} + \left((-1)^n\cos\frac{\theta}{2} + 1\right) H_{\frac{n}{2} \pm \frac{\theta}{4\pi} - \frac{1}{2}} \right) \tilde{W}\left(\omega - (2n-1)\Omega\right) \Bigg],
\end{aligned} \tag{12}$$

where $\tilde{W}$ is the Fourier transform of the window function (i.e., a regularized delta function), H_n is the harmonic number, $\mathrm{Re}\,\sigma = \pi\frac{(\Delta/2)^2}{eE_0}[1 + \mathcal{O}(\gamma^2)]$, and $\theta = \frac{4eE_0}{\hbar\Omega^2}[1 + \mathcal{O}(\gamma^2)]$.

The analytic formula (12) captures the important features of the exact numerical results for small γ; see Fig. 3.

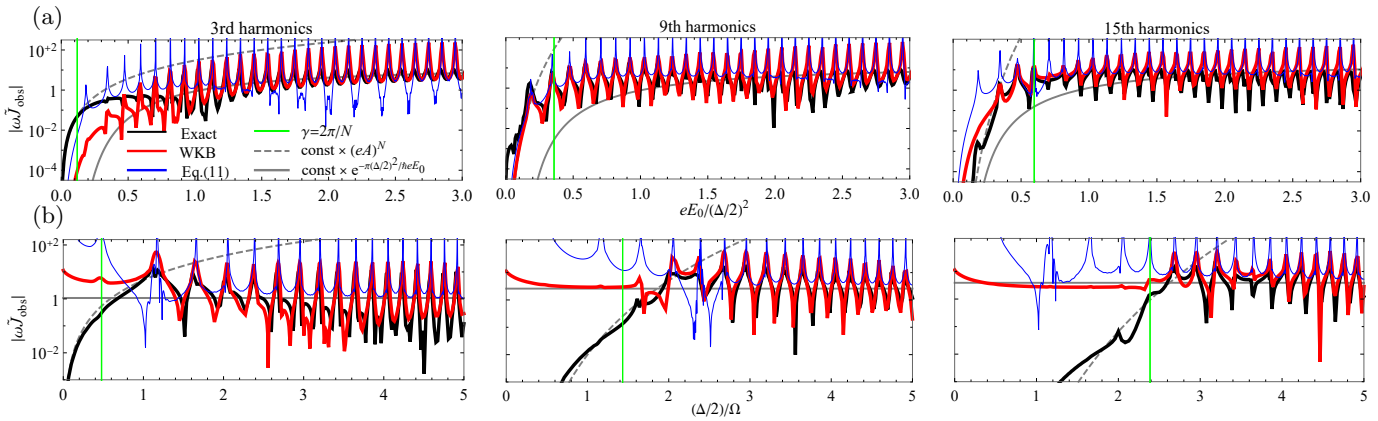


FIG. 3. The magnitude of $N = 3$ (left), 9 (middle), and 15 (right) harmonic peaks plotted against amplitude eE_0 with fixed frequency $\Omega/(\Delta/2) = 1/4$ (a) and inverse frequency Ω^{-1} with fixed amplitude $eE_0/(\Delta/2)^2 = 1$ (b). The other parameters are chosen as $\Omega t_{\rm in} = -17\pi/3$, $T_w = 2|t_{\rm in}|$.

The saturation behavior is determined by the overall factor $\mathrm{e}^{-\frac{\mathrm{Re}\,\sigma}{\hbar}}$, reflecting the abundance of pair production due to tunneling. The oscillating behavior derives from $\cos\frac{\theta}{2}$ in the denominators. Whenever θ hits an odd-integer multiple of π, each harmonic intensity is maximized, as anticipated from the quantum-interference argument. Incidentally, the second terms in the square brackets give odd-order harmonics, while the first ones give non-integer split peaks around integer harmonics with $\delta N = \pm\theta/\pi$. This splitting is a transient effect, as is evident from the $t_{\rm in}$-dependence, and is tunable by changing the Stückelberg phase θ, which can be varied, e.g., with the carrier-envelop phase [92].

Summary.— We have studied HHG in a massive Dirac system based on the lowest-order WKB approximation, including Stokes phenomena. We have shown that the WKB approximation provides a powerful analytical framework to study HHG in the nonperturbative low-frequency and high-intensity regime and well reproduces the exact results of TDSE. Our results imply that the repetitive dynamics of production and acceleration of electron-hole pairs and quantum interference due to the Stückelberg phase are the essence of HHG. We have also predicted some characteristic features of HHG in the deep nonperturbative regime, such as the scaling of the cutoff $N_{\rm cut} \propto eE_0/\Omega^2$, the oscillation of harmonic intensities with a period determined by the Stückelberg phase $\theta \propto eE_0/\Omega^2$, and the non-integer splittings of harmonic peaks $\delta N \propto \theta$ as a transient effect. Our WKB approach applies to various media such as Dirac/Weyl materials (including QED), topological insulators, semiconductors, and graphene, paving the way toward a universal understanding of HHG beyond gases.

Acknowledgments.— The authors thank the Yukawa Institute for Theoretical Physics at Kyoto University, where this work was initiated during YITP-T-20-05 The Schwinger Effect and Strong-Field Physics Workshop. H.T. thanks Antonino Di Piazza for useful discussions. M.H. was supported by the US Department of Energy, Office of Science, Office of Nuclear Physics under Award No. DE-FG0201ER41195. T.N.I. was supported by JSPS KAKENHI Grant Nos. JP18K13495 and JP21K13852.

[1] T. Brabec and F. Krausz, Intense few-cycle laser fields: Frontiers of nonlinear optics, Reviews of Modern Physics **72**, 545 (2000).
[2] M. Ferray, A. LHuillier, X. F. Li, L. A. Lompre, G. Mainfray, and C. Manus, Multiple-harmonic conversion of 1064 nm radiation in rare gases, Journal of Physics B: Atomic, Molecular and Optical Physics **21**, L31 (1988).
[3] P. B. Corkum, Plasma perspective on strong field multiphoton ionization, Phys. Rev. Lett. **71**, 1994 (1993).
[4] M. Lewenstein, P. Balcou, M. Y. Ivanov, A. L'Huillier, and P. B. Corkum, Theory of high-harmonic generation by low-frequency laser fields, Phys. Rev. A **49**, 2117 (1994).
[5] P. Heissler, E. Lugovoy, R. Hörlein, L. Waldecker, J. Wenz, M. Heigoldt, K. Khrennikov, S. Karsch, F. Krausz, B. Abel, and G. D. Tsakiris, Using the third state of matter: high harmonic generation from liquid targets, New Journal of Physics **16**, 113045 (2014).
[6] T. T. Luu, Z. Yin, A. Jain, T. Gaumnitz, Y. Pertot, J. Ma, and H. J. Wörner, Extremeultraviolet highharmonic generation in liquids, Nature Communications **9**, 3723 (2018).
[7] S. Ghimire, A. D. DiChiara, E. Sistrunk, P. Agostini, L. F. DiMauro, and D. A. Reis, Observation of high-order harmonic generation in a bulk crystal, Nature physics **7**, 138 (2011).
[8] O. Schubert, M. Hohenleutner, F. Langer, B. Urbanek, C. Lange, U. Huttner, D. Golde, T. Meier, M. Kira, S. W. Koch, *et al.*, Sub-cycle control of terahertz high-harmonic generation by dynamical bloch oscillations, Nature photonics **8**, 119 (2014).
[9] M. Hohenleutner, F. Langer, O. Schubert, M. Knorr,

U. Huttner, S. W. Koch, M. Kira, and R. Huber, Real-time observation of interfering crystal electrons in high-harmonic generation, Nature **523**, 572 (2015).
[10] T. T. Luu, M. Garg, S. Y. Kruchinin, A. Moulet, M. T. Hassan, and E. Goulielmakis, Extreme ultraviolet high-harmonic spectroscopy of solids, Nature **521**, 498 (2015).
[11] K. Kaneshima, Y. Shinohara, K. Takeuchi, N. Ishii, K. Imasaka, T. Kaji, S. Ashihara, K. L. Ishikawa, and J. Itatani, Polarization-Resolved Study of High Harmonics from Bulk Semiconductors, Physical Review Letters **120**, 243903 (2018).
[12] S. A. Mikhailov and K. Ziegler, Nonlinear electromagnetic response of graphene: frequency multiplication and the self-consistent-field effects, Journal of Physics: Condensed Matter **20**, 384204 (2008).
[13] I. Al-Naib, J. E. Sipe, and M. M. Dignam, High harmonic generation in undoped graphene: Interplay of inter- and intraband dynamics, Physical Review B **90**, 245423 (2014).
[14] N. Yoshikawa, T. Tamaya, and K. Tanaka, High-harmonic generation in graphene enhanced by elliptically polarized light excitation, Science **356**, 736 (2017).
[15] H. A. Hafez, S. Kovalev, J.-C. Deinert, Z. Mics, B. Green, N. Awari, M. Chen, S. Germanskiy, U. Lehnert, J. Teichert, Z. Wang, K.-J. Tielrooij, Z. Liu, Z. Chen, A. Narita, K. Müllen, M. Bonn, M. Gensch, and D. Turchinovich, Extremely efficient terahertz high-harmonic generation in graphene by hot Dirac fermions, Nature **561**, 507 (2018).
[16] R. Matsunaga, N. Tsuji, H. Fujita, A. Sugioka, K. Makise, Y. Uzawa, H. Terai, Z. Wang, H. Aoki, and R. Shimano, Light-induced collective pseudospin precession resonating with higgs mode in a superconductor, Science **345**, 1145 (2014).
[17] Y. Kawakami, T. Amano, Y. Yoneyama, Y. Akamine, H. Itoh, G. Kawaguchi, H. M. Yamamoto, H. Kishida, K. Itoh, T. Sasaki, S. Ishihara, Y. Tanaka, K. Yonemitsu, and S. Iwai, Nonlinear charge oscillation driven by a single-cycle light field in an organic superconductor, Nature Photonics **12**, 474 (2018).
[18] K. Yonemitsu, Charge Oscillations Emerging after Application of an Intense Light Field to Superconductors on a Dimer Lattice, Journal of the Physical Society of Japan **87**, 124703 (2018).
[19] S. Nakamura, K. Katsumi, H. Terai, and R. Shimano, Nonreciprocal terahertz second harmonic generation in superconducting nbn under supercurrent injection, arXiv (2020).
[20] Y. Murakami, M. Eckstein, and P. Werner, High-Harmonic Generation in Mott Insulators, Physical Review Letters **121**, 057405 (2018).
[21] S. Imai, A. Ono, and S. Ishihara, High Harmonic Generation in a Correlated Electron System, Physical Review Letters **124**, 10.1103/PhysRevLett.124.157404 (2020), arXiv:1907.05687.
[22] M. Lysne, Y. Murakami, and P. Werner, Signatures of bosonic excitations in high-harmonic spectra of Mott insulators, Phys. Rev. B **101**, 195139 (2020).
[23] A. Roy, S. Bera, and K. Saha, Nonlinear dynamical response of interacting bosons to synthetic electric field, Physical Review Research **2**, 43133 (2020).
[24] Y. S. You, Y. Yin, Y. Wu, A. Chew, X. Ren, F. Zhuang, S. Gholam-Mirzaei, M. Chini, Z. Chang, and S. Ghimire, High-harmonic generation in amorphous solids, Nature communications **8**, 1 (2017).
[25] P. Jürgens, B. Liewehr, B. Kruse, C. Peltz, D. Engel, A. Husakou, T. Witting, M. Ivanov, M. Vrakking, T. Fennel, *et al.*, Origin of strong-field-induced low-order harmonic generation in amorphous quartz, Nature Physics **16**, 1035 (2020).
[26] G. Vampa, T. J. Hammond, N. Thiré, B. E. Schmidt, F. Légaré, C. R. McDonald, T. Brabec, D. D. Klug, and P. B. Corkum, All-optical reconstruction of crystal band structure, Phys. Rev. Lett. **115**, 193603 (2015).
[27] A. Di Piazza, K. Z. Hatsagortsyan, and C. H. Keitel, Harmonic generation from laser-driven vacuum, Phys. Rev. D **72**, 085005 (2005).
[28] A. Fedotov and N. Narozhny, Generation of harmonics by a focused laser beam in the vacuum, Physics Letters A **362**, 1 (2007).
[29] U. Huttner, M. Kira, and S. W. Koch, Ultrahigh off-resonant field effects in semiconductors, Laser & Photonics Reviews **11**, 1700049 (2017).
[30] S. Ghimire and D. A. Reis, High-harmonic generation from solids, Nature Physics **15**, 10 (2019).
[31] M. Wu, S. Ghimire, D. A. Reis, K. J. Schafer, and M. B. Gaarde, High-harmonic generation from Bloch electrons in solids, Physical Review A **91**, 043839 (2015).
[32] T. Ikemachi, Y. Shinohara, T. Sato, J. Yumoto, M. Kuwata-Gonokami, and K. L. Ishikawa, Trajectory analysis of high-order-harmonic generation from periodic crystals, Physical Review A **95**, 043416 (2017).
[33] E. N. Osika, A. Chacón, L. Ortmann, N. Suárez, J. A. Pérez-Hernández, B. Szafran, M. F. Ciappina, F. Sols, A. S. Landsman, and M. Lewenstein, Wannier-Bloch Approach to Localization in High-Harmonics Generation in Solids, Physical Review X **7**, 021017 (2017).
[34] D. Golde, T. Meier, and S. W. Koch, High harmonics generated in semiconductor nanostructures by the coupled dynamics of optical inter- and intraband excitations, Physical Review B **77**, 075330 (2008).
[35] D. Golde, M. Kira, T. Meier, and S. W. Koch, Microscopic theory of the extremely nonlinear terahertz response of semiconductors, Physica Status Solidi B **248**, 863 (2011).
[36] G. Vampa, C. R. McDonald, G. Orlando, D. D. Klug, P. B. Corkum, and T. Brabec, Theoretical Analysis of High-Harmonic Generation in Solids, Physical Review Letters **113**, 073901 (2014).
[37] G. Vampa, C. R. McDonald, G. Orlando, P. B. Corkum, and T. Brabec, Semiclassical analysis of high harmonic generation in bulk crystals, Physical Review B **91**, 064302 (2015).
[38] K. A. Pronin, A. D. Bandrauk, and A. A. Ovchinnikov, Harmonic generation by a one-dimensional conductor: Exact results, Physical Review B **50**, 3473 (1994).
[39] T. N. Ikeda, K. Chinzei, and H. Tsunetsugu, Floquet-theoretical formulation and analysis of high-order harmonic generation in solids, Physical Review A **98**, 063426 (2018).
[40] K. Chinzei and T. N. Ikeda, Disorder effects on the origin of high-order harmonic generation in solids, Physical Review Research **2**, 013033 (2020).
[41] G. Wentzel, Eine Verallgemeinerung der Quantenbedingungen fr die Zwecke der Wellenmechanik, Z. Phys. **38**, 518 (1926).
[42] H. Kramers, Wellenmechanik und halbzahlige Quantisierung, Z. Phys. **39**, 828 (1926).

[43] L. Brillouin, La mécanique ondulatoire de Schrödinger; une méthode générale de resolution par approximations successives, Compt. Rend. Hebd. Seances Acad. Sci. **183**, 24 (1926).

[44] H. Jeffreys, On certain approximate solutions of linear differential equations of the second order, Proc. London Math. Soc. **23**, 428 (1924).

[45] A. Voros, The return of the quartic oscillator. The complex WKB method, Annales de l'I.H.P. Physique théorique **39**, 211 (1983).

[46] B. Candelpergher, J. C. Nosmas, and F. Pham, Approche de la résurgence, Actualités mathématiques (1993).

[47] H. Dillinger, E. Delabaere, and F. Pham, Résurgence de Voros et périodes des courbes hyperelliptiques, Annales de l'Institut Fourier **43**, 163 (1993).

[48] E. Delabaere, H. Dillinger, and F. Pham, Exact semiclassical expansions for one-dimensional quantum oscillators, Journal of Mathematical Physics **38**, 6126 (1997).

[49] E. Delabaere and F. Pham, Resurgent methods in semi-classical asymptotics, Annales de l'I.H.P. Physique théorique **71**, 1 (1999).

[50] T. Aoki, T. Kawai, and Y. Takei, The Bender-Wu Analysis and the Voros Theory, ICM-90 Satellite Conference Proceedings , 1 (1991).

[51] T. Aoki, T. Kawai, and Y. Takei, The Bender-Wu Analysis and the Voros Theory II, Advanced Studies in Pure Mathematics **54**, 19 (2009).

[52] T. Aoki, T. Kawai, and Y. Takei, Algebraic analysis of singular perturbations: On exact WKB analysis (1993).

[53] S. Enomoto and T. Matsuda, The exact WKB for cosmological particle production, JHEP **03**, 090, arXiv:2010.14835 [hep-ph].

[54] S. Enomoto and T. Matsuda, The Exact WKB and the Landau-Zener transition for asymmetry in cosmological particle production, (2021), arXiv:2104.02312 [hep-th].

[55] H. Taya, T. Fujimori, T. Misumi, M. Nitta, and N. Sakai, Exact WKB analysis of the vacuum pair production by time-dependent electric fields, JHEP **03**, 082, arXiv:2010.16080 [hep-th].

[56] S. Hashiba and Y. Yamada, Stokes phenomenon and gravitational particle production – How to evaluate it in practice, (2021), arXiv:2101.07634 [hep-th].

[57] C. M. Sou, X. Tong, and Y. Wang, Chemical-Potential-Assisted Particle Production in FRW Spacetimes, (2021), arXiv:2104.08772 [hep-th].

[58] E. Raicher, S. Eliezer, C. H. Keitel, and K. Z. Hatsagortsyan, Semiclassical limitations for photon emission in strong external fields, Phys. Rev. A **99**, 052513 (2019).

[59] A. Di Piazza, Ultrarelativistic electron states in a general background electromagnetic field, Phys. Rev. Lett. **113**, 040402 (2014), arXiv:1310.7856 [hep-ph].

[60] A. Di Piazza, WKB Electron Wave Functions in a Tightly Focused Laser Beam, (2021), arXiv:2102.06692 [hep-ph].

[61] L. V. Keldysh, Ionization in the Field of a Strong Electromagnetic Wave, J. Exp. Theor. Phys. **20**, 1307 (1965).

[62] E. Brezin and C. Itzykson, Pair production in vacuum by an alternating field, Phys. Rev. D **2**, 1191 (1970).

[63] V. S. Popov, Production of e+e- Pairs in an Alternating External Field, JETP Lett. **13**, 185 (1971).

[64] H. Taya, H. Fujii, and K. Itakura, Finite pulse effects on e^+e^- pair creation from strong electric fields, Phys. Rev. D **90**, 014039 (2014), arXiv:1405.6182 [hep-ph].

[65] L. D. Landau, Zur theorie der phasenumwandlungen ii, Phys. Z. Sowjetunion **11**, 26 (1937).

[66] C. Zener, Non-adiabatic crossing of energy levels, Proceedings of the Royal Society of London. Series A, Containing Papers of a Mathematical and Physical Character **137**, 696 (1932).

[67] E. K. G. Stückelberg, *Theorie der unelastischen Stösse zwischen Atomen* (Birkhäuser, 1933).

[68] E. Majorana, Atomi orientati in campo magnetico variabile, Il Nuovo Cimento **9**, 43 (1932).

[69] F. Sauter, Uber das Verhalten eines Elektrons im homogenen elektrischen Feld nach der relativistischen Theorie Diracs, Z. Phys. **69**, 742 (1931).

[70] W. Heisenberg and H. Euler, Consequences of Dirac's theory of positrons, Z. Phys. **98**, 714 (1936), arXiv:physics/0605038.

[71] J. S. Schwinger, On gauge invariance and vacuum polarization, Phys. Rev. **82**, 664 (1951).

[72] When an applied electric field is spatially uniform and linearly polarized, spin degrees of freedom are degenerated no matter what the spacetime dimension is and hence the Dirac Hamiltonian reduces in general to a two-level system, describing the valence- and conduction-band-electrons degrees of freedom.

[73] C. Jürß and D. Bauer, High-harmonic generation in Su-Schrieffer-Heeger chains, Physical Review B **99**, 195428 (2019).

[74] E. McCann and V. I. Fal'ko, Landau-level degeneracy and quantum hall effect in a graphite bilayer, Phys. Rev. Lett. **96**, 086805 (2006).

[75] E. McCann and M. Koshino, The electronic properties of bilayer graphene, Reports on Progress in Physics **76**, 056503 (2013).

[76] Y. L. Chen, J.-H. Chu, J. G. Analytis, Z. K. Liu, K. Igarashi, H.-H. Kuo, X. L. Qi, S. K. Mo, R. G. Moore, D. H. Lu, M. Hashimoto, T. Sasagawa, S. C. Zhang, I. R. Fisher, Z. Hussain, and Z. X. Shen, Massive dirac fermion on the surface of a magnetically doped topological insulator, Science **329**, 659 (2010).

[77] H.-Z. Lu, W.-Y. Shan, W. Yao, Q. Niu, and S.-Q. Shen, Massive dirac fermions and spin physics in an ultrathin film of topological insulator, Phys. Rev. B **81**, 115407 (2010).

[78] B. Cheng, N. Kanda, T. N. Ikeda, T. Matsuda, P. Xia, T. Schumann, S. Stemmer, J. Itatani, N. Armitage, and R. Matsunaga, Efficient Terahertz Harmonic Generation with Coherent Acceleration of Electrons in the Dirac Semimetal Cd3As2, Physical Review Letters **124**, 117402 (2020).

[79] S. Kovalev, R. M. A. Dantas, S. Germanskiy, J.-C. Deinert, B. Green, I. Ilyakov, N. Awari, M. Chen, M. Bawatna, J. Ling, F. Xiu, P. H. M. van Loosdrecht, P. Surówka, T. Oka, and Z. Wang, Non-perturbative terahertz high-harmonic generation in the three-dimensional Dirac semimetal Cd3As2, Nature Communications **11**, 2451 (2020).

[80] C. K. Dumlu and G. V. Dunne, Interference Effects in Schwinger Vacuum Pair Production for Time-Dependent Laser Pulses, Phys. Rev. D **83**, 065028 (2011), arXiv:1102.2899 [hep-th].

[81] C. K. Dumlu and G. V. Dunne, The Stokes Phenomenon and Schwinger Vacuum Pair Production in Time-Dependent Laser Pulses, Phys. Rev. Lett. **104**, 250402 (2010), arXiv:1004.2509 [hep-th].

[82] S. Shevchenko, S. Ashhab, and F. Nori, Landauzenerstckelberg interferometry, Physics Reports **492**, 130 (2010).

[83] N. Tanji, Dynamical view of pair creation in uniform electric and magnetic fields, Annals Phys. **324**, 1691 (2009), arXiv:0810.4429 [hep-ph].
[84] N. D. Birrell and P. C. W. Davies, *Quantum Fields in Curved Space*, Cambridge Monographs on Mathematical Physics (Cambridge Univ. Press, Cambridge, UK, 1984).
[85] S. A. Mikhailov, Non-linear electromagnetic response of graphene, Europhysics Letters (EPL) **79**, 27002 (2007).
[86] L. Yue and M. B. Gaarde, Expanded View of Electron-Hole Recollisions in Solid-State High-Harmonic Generation: Significance of the Full Brillouin Zone, arXiv:2102.11964 (2021), arXiv:2102.11964.
[87] T. N. Ikeda, High-order nonlinear optical response of a twisted bilayer graphene, Phys. Rev. Research **2**, 032015 (2020).
[88] See Supplemental Material.
[89] E. S. Toma, P. Antoine, A. De Bohan, and H. G. Muller, Resonance-enhanced high-harmonic generation, Journal of Physics B: Atomic, Molecular and Optical Physics **32**, 5843 (1999).
[90] S. V. Popruzhenko, P. A. Korneev, S. P. Goreslavski, and W. Becker, Laser-Induced Recollision Phenomena: Interference Resonances at Channel Closings, Physical Review Letters **89**, 23001 (2002).
[91] P. Xia, T. Tamaya, C. Kim, F. Lu, T. Kanai, N. Ishii, J. Itatani, H. Akiyama, and T. Kato, High-harmonic generation in gaas beyond the perturbative regime (2020), arXiv:2004.04492 [cond-mat.mes-hall].
[92] C. P. Schmid, L. Weigl, P. Grössing, V. Junk, C. Gorini, S. Schlauderer, S. Ito, M. Meierhofer, N. Hofmann, D. Afanasiev, J. Crewse, K. A. Kokh, O. E. Tereshchenko, J. Güdde, F. Evers, J. Wilhelm, K. Richter, U. Höfer, and R. Huber, Tunable non-integer high-harmonic generation in a topological insulator, Nature **593**, 385 (2021).